

Photochemical Mechanisms Responsible for the Versatile Application of Naphthalimides and Naphthalaldimides in Biological Systems

Béatrice M. Aveline,[†] Seiichi Matsugo,[‡] and Robert W. Redmond^{*,†}

Contribution from the Wellman Laboratories of Photomedicine, Harvard Medical School, Massachusetts General Hospital, Boston, Massachusetts 02114, and Department of Chemical and Biochemical Engineering, Faculty of Engineering, Toyama University, Gofuku 3190, Toyama 930, Japan

Received June 20, 1997[©]

Abstract: Despite the number and variety of their biological applications, the mechanisms of action of the photoactive naphthalenic imides have not yet been fully elucidated. In order to provide mechanistic insight, the photochemistry of several *N*-substituted 1,8-naphthalimides (NI) and 1,4,5,8-naphthalaldimides (NDI) has been studied using absorption and fluorescence spectroscopy and by laser flash photolysis ($\lambda_{\text{exc}} = 355 \text{ nm}$). The lowest singlet state (S_1) is mainly $\pi\pi^*$ in nature for NI whereas $n\pi^*$ character predominates for the NDI. This difference exerts a profound effect on subsequent reaction mechanisms: upon irradiation, only the NDI molecules can undergo intramolecular γ hydrogen abstraction. In the case of NP-III, a bishydroperoxy NDI derivative, this photoprocess ($\Phi = 0.03$) leads to concomitant formation of an oxygen-centered radical ($\epsilon = 21\,600 \text{ M}^{-1} \text{ cm}^{-1}$ at 465 nm in acetonitrile) and release of the hydroxyl radical ($\cdot\text{OH}$). All the compounds studied produce the triplet state (in acetonitrile, $\epsilon_T \approx 10\,500\text{--}11\,500 \text{ M}^{-1} \text{ cm}^{-1}$ at 470 nm for NI and 485 nm for NDI). The quantum yield of intersystem crossing was determined to be close to unity except where intramolecular γ hydrogen abstraction was possible ($\Phi_{\text{isc}} < 0.5$). The triplet states were found to efficiently sensitize the formation of singlet oxygen (with $S_{\Delta} > 0.8$ for NI and > 0.5 for NDI). In the absence of quenchers, the triplet states react with the ground-state of starting material *via* electron-transfer with a high rate constant [$k = (4\text{--}6) \times 10^9$ and $5 \times 10^8 \text{ M}^{-1} \text{ s}^{-1}$ for NDI and NI, respectively] to give the radical anion and radical cation of the corresponding naphthalenic derivative. The high reactivity of the triplet states toward electron donors such as DABCO and their low ability for hydrogen abstraction are typical of a $\pi\pi^*$ configuration. These mechanistic photochemistry results are discussed with regard to the photobiological effects observed for these compounds and show that the actual reaction leading to biological damage will depend on the microenvironment of the naphthalenic molecule.

Naphthalenic imides constitute a very versatile class of compounds which have been used in a large variety of areas. Their most recent applications have been oriented toward the fields of biology and medicine. Substituted 1,8-naphthalimides and bisnaphthalimides¹ have been shown to demonstrate dramatic anticancer activity,^{2,3} and members of both series have already entered into clinical trials.⁴ Although the precise mechanism of their tumoricidal efficacy has not yet been fully understood, several lines of evidence suggest that it is linked to their ability to intercalate into DNA with high affinity and sequence specificity.⁵ Sulfonated naphthalimides and bisnaphthalimides have also been reported to be very promising antiviral agents with selective *in vitro* activity against the human immunodeficiency virus, HIV-1.⁶

In addition to the above "dark" properties, photochemical activation of these naphthalenic derivatives has been used to further broaden the range of biological applications. In this respect, brominated mono- and bisnaphthalimides have been proposed as good candidates for the photochemotherapeutic

inhibition of enveloped viruses in blood and blood products.^{7–9} Photoexcitation of the bichromophoric derivatives has also been found to efficiently induce cross-linking of proteins such as collagen.^{10–12} This property has led to the investigation of their

(4) (a) Saez, R.; Craig, J. B.; Kuhn, J. G.; Weiss, G. R.; Koeller, J.; Phillips, J.; Havlin, K.; Harmon, G.; Hardy, J.; Melink, T. J.; Sarosy, G. A.; Van Hoff, D. *J. Clin. Oncol.* **1989**, *7*, 1351–1358. (b) Llobart, M.; Poveda, A.; Forner, E.; Fernandez-Martos, C.; Gasper, C.; Munoz, M.; Olmos, T.; Ruiz, A.; Soriano, V.; Benarides, A.; Martin, M.; Schlik, E.; Guillem, V. *Invest. New Drugs* **1992**, *10*, 177–181. (c) Malviya, V. K.; Liu, P. Y.; Alberts, D. S.; Surwit, E. A.; Craig, J. B.; Hanningan, E. V. *Am. J. Clin. Oncol.* **1992**, *15*, 41–44. (d) Cobb, P. W.; Degen, D. R.; Clark, G. M.; Chen, S.-F.; Kuhn, J. G.; Gross, J. L.; Kirshenbaum, M. R.; Sun, J.-H.; Burris, H. A., III; Von Hoff, D. D. *J. Natl. Cancer Inst.* **1994**, *86*, 1462–1465. (e) McRipley, R. J.; Burns-Horwitz, P. E.; Czerniak, P. M.; Diamond, R. J.; Diamond, M. A.; Miller, J. L. D.; Page, R. J.; Dexter, D. L.; Chen, S.-F.; Sun, J.-H.; Behrens, C. H.; Seitz, S. P.; Gross, J. L. *Cancer Res.* **1994**, *54*, 159–163. (f) Kirshenbaum, M. R.; Chen, S.-F.; Behrens, C. H.; Papp, L. M.; Stafford, M. M.; Sun, J.-H.; Behrens, D. L.; Fredericks, J. R.; Polkus, S. T.; Sipple, P.; Patten, A. D.; Dexter, D. L.; Seitz, S. P.; Gross, J. L. *Cancer Res.* **1994**, *54*, 2199–2206. (g) Bousquet, P. F.; Brana, M. F.; Conlon, D.; Fitzgerald, K. M.; Perron, D.; Cocchiario, C.; Miller, R.; Moran, M.; George, J.; Qian, X.-D.; Keilhauer, G.; Romerdahl, C. A. *Cancer Res.* **1995**, *55*, 1176–1180.

(5) Waring, M. J.; Gonzalez, A.; Jimenez, A.; Vazquez, D. *Nucleic Acids Res.* **1979**, *7*, 217–233.

(6) Rideout, D.; Schinazi, R.; Pauza, C. D.; Lovelace, K.; Chiang, L.-C.; Calogeropoulou, T.; McCarthy, M.; Elder, J. H. *J. Cell. Biochem.* **1993**, *51*, 446–457.

(7) Chanh, T. C.; Lewis, D. E.; Allan, J. S.; Sogandares-Bernal, F.; Judy, M. M.; Utecht, R. E.; Matthews, J. L. *AIDS Res. Hum. Retroviruses* **1993**, *9*, 891–896.

(8) Chanh, T. C.; Archer, B. J.; Utecht, R. E.; Lewis, D. E.; Judy, M. M.; Matthews, J. L. *Biomed. Chem. Lett.* **1993**, *3*, 555–556.

[†] Harvard Medical School.

[‡] Toyama University.

[©] Abstract published in *Advance ACS Abstracts*, November 1, 1997.

(1) (a) These molecules are formed by connecting two chromophore units with a chemical bridge. (b) Brana, M. F.; Castellano, J. M.; Moran, M.; Perez de Vega, M. J.; Romerdahl, C. R.; Qian, X.-D.; Bousquet, P.; Emling, F.; Schlick, E. *Anti-Cancer Drug Design* **1993**, *8*, 257–268.

(2) Brana, M. F.; Castellano, J. M.; Roldan, C. M.; Santos, A.; Vazquez, D.; Jimenez, A. *Cancer Chemother. Pharmacol.* **1980**, *4*, 61–66.

(3) Brana, M. F.; Castellano, J. M.; Sanz, A. M.; Roldan, C. M.; Roldan, C. *Eur. J. Med. Chem.* **1981**, *16*, 207–212.

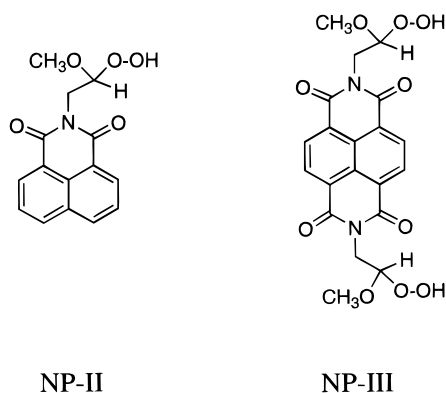


Figure 1. Chemical structures of *N*-(2-hydroperoxy-2-methoxyethyl)-1,8-naphthalimide (NP-II) and *N,N'*-bis(2-hydroperoxy-2-methoxyethyl)-1,4,5,8-naphthalaldhiimide (NP-III).

potential application in light-induced tissue-repair and welding of meniscal cartilage, articular cartilage and cornea has been achieved *in vitro*.^{13,14} The combination of high photoactivity and DNA-intercalation has also prompted the use of some naphthalenic derivatives as sequence-specific DNA-photocleavages.¹⁵ Depending on the chemical structure of the compound used, various mechanisms have been proposed, involving free radical formation,¹⁶ photogeneration of carbocation,¹⁷ electron-transfer from oxidizable guanine residues (G),¹⁸ or hydrogen abstraction from thymine,¹⁹ but a lack of experimental evidence precludes the confirmation of these proposals.

The most intriguing molecules of this family are the hydroperoxy derivatives NP-II and NP-III (presented in Figure 1), which have been designed with the goal of generating the hydroxyl radical ($\cdot\text{OH}$) upon near-UV irradiation and named "photo-Fenton reagents".^{20,21} Photoexcitation of these compounds has been shown to cause DNA-strand breaks^{20,21} and in the case of the naphthalaldhiimide (NP-III), a sequence-specific cleavage at the 5'G of 5'-GG-3' sites has been observed.^{21,22} NP-III has also been used to investigate oxidative modifications induced by $\cdot\text{OH}$ in cells,^{23,24} in the eye lens proteins²⁵ and in

the apolipoproteins of human low density lipoprotein (LDL)²⁶ and bovine serum albumin (BSA).²⁷ This compound is important considering the lack of convenient sources for the study of $\cdot\text{OH}$ reactions in biologically relevant systems^{28,29} and the general effort put into the development of new, selective photochemical $\cdot\text{OH}$ generators.³⁰⁻⁴¹

We report here the results of a study of the photochemistry of the bishydroperoxy naphthalaldhiimide, NP-III, and related molecules. In order to elucidate the potential bioreactivity of NP-III, it was necessary to investigate the structural effects (nature of the substituent on the nitrogen atom, mono- or bifunctionality of the molecule) on the primary and subsequent photochemistry of these compounds. In this manner, we have demonstrated a variety of possible mechanisms by which photoactivation of NP-III could result in biological damage and shown that the exact mechanism in operation will depend on the microenvironment of the excited molecule.

Experimental Section

Chemicals. All reagents used were supplied by Sigma Chemical Co. (St. Louis, MO), Fisher Chemical (Pittsburgh, PA) or Aldrich Chemical Co. (Milwaukee, WI). Organic solvents were of spectroscopic grade from Fisher, deuterated acetonitrile (CD_3CN : 99.6 atom % D) was from Aldrich and Phosphate Buffered Saline Salt Solution (PBS, pH = 7.2) was purchased from Gibco BRL (Grand Island, NY).

Figures 1 and 2 show the chemical structures of the naphthalimide and naphthalaldhiimide derivatives studied. 1,8-Naphthalimide (**1**) was provided by Aldrich and used as supplied. NP-II, NP-III, and compounds **2** and **3** were synthesized and purified as previously described.^{20,25,42} All the naphthalenic derivatives were stored in solid form at -20°C . Solutions were prepared immediately before use and were protected from light at all times. In case of low hydrophilicity, a concentrated solution of naphthalenic derivative in acetonitrile was diluted with PBS (the pH of the resulting solution was verified to be 7.2, and the percentage by volume of acetonitrile in the final sample was <1%).

General Techniques. Ground-state absorption properties were studied using a Cary 2300 UV-visible spectrophotometer or a Hewlett-

(24) Matsugo, S.; Kodaira, K. I.; Saito, I. *Bioorg. Med. Chem. Lett.* **1993**, *3*, 1571.

(25) Guptasarma, P.; Balasubramanian, D.; Matsugo, S.; Saito, I. *Biochemistry* **1992**, *31*, 4296-4303.

(26) Matsugo, S.; Yan, L.-J.; Packer, L. *Biochem. Biophys. Res. Commun.* **1995**, *206*, 138-145.

(27) Matsugo, S.; Yan, L.-J.; Trischler, H. J.; Packer, L. *Biochem. Biophys. Res. Commun.* **1995**, *208*, 161-167.

(28) Halliwell, B.; Gutteridge, J. M. C. *Free Radicals in Biology and Medicine*; Oxford University Press: Oxford, 1989.

(29) Bensasson, R. V.; Land, E. J.; Truscott, T. G. *Excited States and Free Radicals in Biology and Medicine*; Oxford University Press: Oxford, 1993.

(30) Saito, I.; Takayama, M.; Matsuura, T.; Matsugo, S.; Kawanishi, S. *J. Am. Chem. Soc.* **1990**, *112*, 883-884.

(31) Boivin, J.; Elizabeth, C.; Zard, S. Z. *Tetrahedron Lett.* **1990**, *31*, 6869-6872.

(32) Sako, M.; Nagai, K.; Maki, Y. *J. Chem. Soc. Chem. Commun.* **1993**, 750-751.

(33) Adam, W.; Ballmaier, D.; Epe, B.; Grimm, G. N.; Saha-Mölller, C. R. *Angew. Chem., Int. Ed. Engl.* **1995**, *34*, 2156-2158.

(34) Adam, W.; Cadet, J.; Dall'Acqua, F.; Epe, B.; Ramaiah, D.; Saha-Mölller, C. R. *Angew. Chem., Int. Ed. Engl.* **1995**, *34*, 107-110.

(35) Aveline, B. M.; Kochevar, I. E.; Redmond, R. W. *J. Am. Chem. Soc.* **1996**, *118*, 10113-10123.

(36) Aveline, B. M.; Kochevar, I. E.; Redmond, R. W. *J. Am. Chem. Soc.* **1996**, *118*, 289-290.

(37) Aveline, B. M.; Kochevar, I. E.; Redmond, R. W. *J. Am. Chem. Soc.* **1996**, *118*, 10124-10133.

(38) Epe, B.; Ballmaier, D.; Adam, W.; Grimm, G. N.; Sara-Möller, C. R. *Nucleic Acids Res.* **1996**, *24*, 1625-1631.

(39) Saito, I. *Pure Appl. Chem.* **1992**, *64*, 1305-1310.

(40) Saito, I.; Nakatani, K. *Bull. Chem. Soc. Jpn.* **1996**, *69*, 3007-3019.

(41) Möller, M.; Stopper, H.; Häring, M.; Schleger, Y.; Epe, B.; Adam, W.; Saha-Mölller, C. R. *Biochem. Biophys. Res. Commun.* **1995**, *216*, 693-701.

(42) Matsugo, S.; Saito, I. *Tetrahedron Lett.* **1991**, *32*, 2949-2950.

(9) Chanh, T. C.; Lewis, D. E.; Judy, M. M.; Sogandares-Bernal, F.; Michalek, G. R.; Utecht, R. E.; Skiles, H.; Chang, S. C.; Matthews, J. L. *Antiviral Res.* **1994**, *25*, 133-146.

(10) Judy, M. M.; Matthews, J. L.; Boriak, R. L.; Berlacu, A.; Lewis, D. E.; Utecht, R. E. *Proc. Int. Conf. Lasers* **1993**, *15*, 774-776.

(11) Judy, M. M.; Matthews, J. L.; Boriak, A.; Burlacu, A. *Proc. SPIE-Int. Soc. Opt. Eng.* **1993**, *1882*, 305-308.

(12) Judy, M. M.; Fuh, L.; Matthews, J. L.; Lewis, D. E.; Utecht, R. *Proc. SPIE-Int. Soc. Opt. Eng.* **1994**, *2128*, 506-509.

(13) Judy, M. M.; Matthews, J. L.; Boriak, R. L.; Burlacu, A.; Lewis, D. E.; Utecht, R. E. *Proc. SPIE-Int. Soc. Opt. Eng.* **1993**, *1876*, 175-179.

(14) Judy, M. M.; Nosir, H.; Jackson, R. W.; Matthews, J. L.; Lewis, D. E.; Utecht, R. E.; Yuan, D. *Proc. SPIE-Int. Soc. Opt. Eng.* **1996**, *2671*, 251-255.

(15) Bailly, C.; Brana, M.; Waring, M. J. *Eur. J. Biochem.* **1996**, *240*, 195-208.

(16) Mehrotra, J.; Misra, K.; Mishra, R. K. *Nucleosides Nucleotides* **1994**, *13*, 963-978.

(17) Saito, I.; Takayama, M.; Sakurai, T. *J. Am. Chem. Soc.* **1994**, *116*, 2653-2654.

(18) Saito, I.; Takayama, M.; Suyiyama, H.; Nakatani, K. *J. Am. Chem. Soc.* **1995**, *117*, 6406-6407.

(19) Saito, I.; Takayama, M.; Kawanishi, S. *J. Am. Chem. Soc.* **1995**, *117*, 5590-5591.

(20) Matsugo, S.; Saito, I. *Nucleic Acids Res. Symp. Ser.* **1990**, *22*, 57-58.

(21) Matsugo, S.; Miyahara, T.; Yamaguchi, K.; Mori, T.; Saito, I. *Nucleic Acids Res. Symp. Ser.* **1991**, *21*, 109-110.

(22) Matsugo, S.; Kawanishi, S.; Yamamoto, K.; Sugiyama, H.; Matsuura, T.; Saito, I. *Angew. Chem., Int. Ed. Engl.* **1991**, *30*, 1351-1353.

(23) Matsugo, S.; Kumaki, S.; Shimasaki, C.; Mori, T.; Saito, I. *Chem. Lett.* **1993**, 453-456.

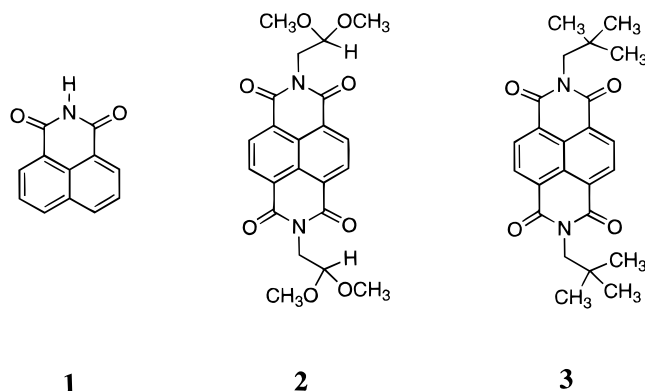


Figure 2. Chemical structures of 1,8-naphthalimide (**1**), *N,N'*-bis(2,2-dimethoxyethyl)-1,4,5,8-naphthalidiimide (**2**), and *N,N'*-bis(2,2-dimethylpropyl)-1,4,5,8-naphthalidiimide (**3**).

Packard HP8451A UV-visible diode array spectrophotometer. Corrected steady-state emission spectra were recorded with a Fluoromax spectrofluorimeter (Spex Industry, Edison, NJ). Fluorescence quantum yields (Φ_f) were determined at $\lambda_{exc} = 330$ nm with quinine bisulfate ($\Phi_f = 0.55$ in 0.5 M sulfuric acid)⁴³ as reference. Standard and samples in air-saturated solutions had absorbances below 0.05. Fluorescence quantum yields were calculated using the following relationship:

$$\Phi_{f(S)} = \Phi_{f(R)}(F_S n_S^2 / F_R n_R^2) \quad (1)$$

where the S subscript refers to the sample and R to the reference. F represents the slope of the integrated area under the emission band versus the absorbance of the solution at 330 nm, and n is the index of refraction at the sodium D line at 20 °C.

Laser Flash Photolysis. The nanosecond laser flash photolysis apparatus has been described in detail elsewhere.^{44,45} For most of the experiments, excitation was provided by the frequency-tripled output of a Quantel YG660 Nd:YAG laser (355 nm, 8 ns duration pulse). Laser intensities were attenuated to ≤ 18 mJ cm⁻² pulse⁻¹ through the use of neutral density filters. Quenching rate constants were measured using static samples. Transient absorption spectra and kinetic signals under aerated conditions were recorded using a flow system ensuring irradiation of a completely fresh volume of solution with each laser pulse. When nitrogen- or oxygen-saturated conditions were needed, experiments were carried out with a static sample which was shaken between laser shots. The samples were contained in a 10 mm \times 10 mm quartz cuvette. Photosensitization experiments were performed using the frequency-quadrupled output of the Nd:YAG laser (266 nm, 8 ns duration pulse, up to 10 mJ cm⁻² pulse⁻¹).

Molar absorption coefficients of the triplet states (ϵ_T) of naphthalenic derivatives were obtained by the sensitization method. Pulsed excitation ($\lambda_{exc} = 266$ nm) of 4-methoxyacetophenone in the presence of naphthalimide or naphthalidiimide is followed by energy transfer to form the triplet state of the acceptor molecule.⁴⁶ Under the conditions employed for these experiments, the light was absorbed predominantly by the sensitizer ($\geq 90\%$).⁴⁷ The ϵ_T values were determined using the following relationship:

(43) Melhuish, W. H. *J. Phys. Chem.* **1961**, *65*, 229.

(44) Krieg, M.; Srichai, M. B.; Redmond, R. W. *Biochem. Biophys. Acta* **1993**, *1151*, 168–174.

(45) Aveline, B.; Hasan, T.; Redmond, R. W. *Photochem. Photobiol.* **1994**, *59*, 328–335.

(46) This method is based on the assumption that the triplet state of 4-MAP is exclusively quenched by energy transfer. No electron transfer between ³(4-MAP)* and the naphthalenic derivatives was observed.

(47) To correct for the absorbance due to direct excitation of the naphthalimide or naphthalidiimide, two sets of experiments were carried out: one for the naphthalenic derivative alone in solution (where a small amount of triplet state is generated by direct excitation) and the other one in the presence of sensitizer (where further naphthalenic triplet state is produced by sensitization). The $\Delta A_{T_{obs}}$ value used in eq 3 was calculated as the differential between the ΔA values obtained from these two experiments.

$$\epsilon_T = \epsilon_{T(D)}(\Delta A_T / \Delta A_{T(D)}) \quad (2)$$

where $\epsilon_{T(D)}$ is the molar absorption coefficient of the triplet state of the sensitizer,⁴⁸ $\Delta A_{T(D)}$ is the maximum absorbance of the triplet donor in the absence of the acceptor and ΔA_T is the sensitized triplet absorbance of the naphthalimide or naphthalidiimide studied. This latter value corresponds to the observed triplet absorbance ($\Delta A_{T_{obs}}$) corrected for underestimation due to incomplete ($< 100\%$) quenching of sensitizer triplet states by the naphthalenic derivative. This correction was carried out using

$$\Delta A_T = \Delta A_{T_{obs}} k_{obs} / (k_{obs} - k_1) \quad (3)$$

where k_1 and k_{obs} are the rate constants for the decay of the triplet state of the sensitizer in the absence and in the presence of the acceptor molecule, respectively (k_{obs} is given by eq 4, where k_{ET} is the bimolecular rate constant for triplet energy transfer from the sensitizer to the naphthalenic derivative, N). This correction was never greater than 10%.

$$k_{obs} = k_1 + k_{ET}[N] \quad (4)$$

Quantum yields (Φ) of photoprocesses undergone by the naphthalenic molecules were determined by comparative actinometry as previously described,^{35,49} using benzophenone in deaerated benzene (for which $\Phi_{isc} = 1.0$ ⁵⁰ and $\epsilon_T = 7220$ M⁻¹ cm⁻¹ at 530 nm⁵¹) as standard.

Photoconductivity. Transient photoconductivity measurements were performed with samples contained in a 10 mm \times 10 mm path length quartz cuvette equipped with a Teflon insert holding three horizontal platinum foil electrodes (4 \times 4 mm²) spaced exactly 4 mm apart. The volume between the common center electrode and one of the outer electrodes was excited by the laser beam whereas the unirradiated volume between the other outer electrode and the common provided a measure of the background signal. A DC voltage pulse, of variable duration (1–4 ms) and amplitude (≤ 400 V), was applied across the electrodes, prior to the laser pulse. Signals were taken to a differential amplifier to increase the signal to noise and observe only photoinduced changes in conductivity of the sample. The differential signal was passed to the digital oscilloscope and processed as in the laser flash photolysis experiments. The electrode arrangement was such that optical and conductivity detection could be carried out on the same sample.

Infrared Luminescence. Singlet oxygen (O_2 (¹ Δ_g)) formation was detected using the time-resolved infrared luminescence technique using a (EOSS G-050) germanium diode-based system,^{52,53} equipped with a Judson PA-100 pre-amplifier. Singlet oxygen quantum yields (Φ_Δ) were calculated by comparison of the slopes of the linear energy dependence plots of the maximum luminescence emission obtained for the naphthalenic derivatives and phenazine used as reference ($\Phi_\Delta = 0.84$ ⁵⁴). Standard and samples in air-saturated deuterated acetonitrile were optically matched at $\lambda_{exc} = 355$ nm.

Cyclic Voltammetry. The reduction potentials ($E_{1/2}^{red}$) of the naphthalenic derivatives were measured in anhydrous acetonitrile containing ≤ 1 mM naphthalimide or naphthalidiimide and 0.1 M tetra-*n*-butylammonium fluoroborate (TBAF). Solutions were bubbled with nitrogen

(48) (a) $\epsilon_{T(D)}$ for 4-methoxyacetophenone (4-MAP) in acetonitrile was determined to be 16 100 M⁻¹ cm⁻¹ at 380 nm by comparative actinometry using benzophenone in deaerated acetonitrile (for which $\Phi_{isc} = 1$ and $\epsilon_T = 6250$ M⁻¹ cm⁻¹ at 530 nm)^{48b} as standard and assuming a triplet state quantum yield of unity for 4-MAP. (b) Murov, S. L.; Carmichael, I.; Hug, G. L. *Handbook of Photochemistry*, 2nd ed.; Marcel Dekker, Inc.: New York, 1993.

(49) Bensasson, R. V.; Land, E. J. *Trans. Faraday Soc.* **1971**, *67*, 1904–1915.

(50) Inbar, S.; Linschitz, H.; Cohen, S. G. *J. Am. Chem. Soc.* **1981**, *103*, 1048–1054.

(51) Hurlley, J. K.; Sinai, N.; Linschitz, H. *Photochem. Photobiol.* **1983**, *38*, 9–14.

(52) Rodgers, M. A. J.; Snowden, P. T. *J. Am. Chem. Soc.* **1982**, *104*, 5541–5543.

(53) Keene, J. P.; Kessel, D.; Land, E. P.; Redmond, R. W.; Truscott, T. G. *Photochem. Photobiol.* **1986**, *43*, 117–120.

(54) Redmond, R. W.; Braslavsky, S. E. *NATO Adv. Study Inst. Photosensitisation: Molecular, Cellular and Medical Aspects* **1988**, *H15*, 93–95.

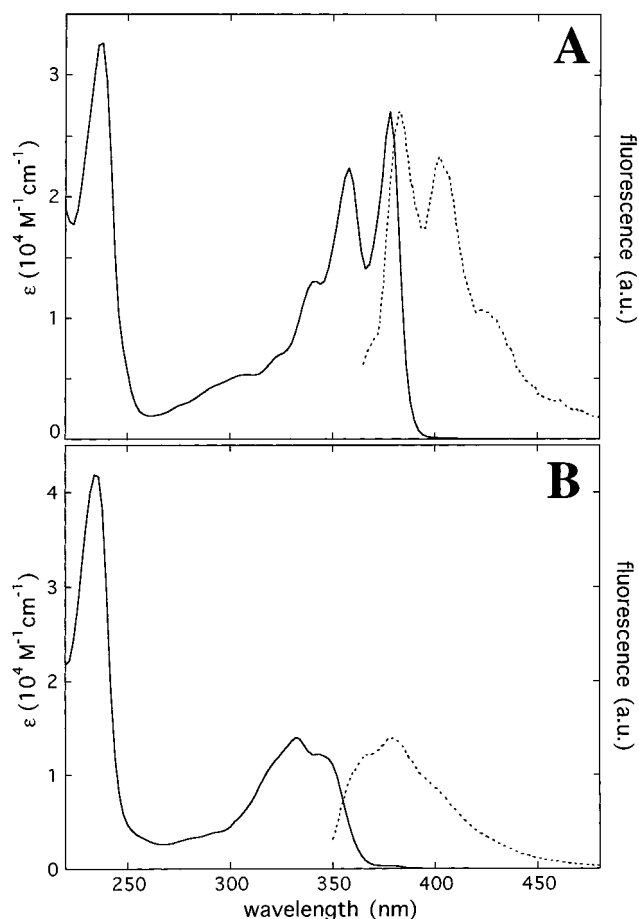


Figure 3. Ground-state absorption (—) and fluorescence emission (---) spectra of NP-III (A) and NP-II (B) in acetonitrile. The emission spectra were recorded under air-saturated conditions using $\lambda_{\text{exc}} = 330$ nm.

prior to the measurement. The cyclic voltammograms were obtained using a potentiostat (model 273, EG&G Princeton Applied Research) coupled to a recorder (model RE0091, EG&G Princeton Applied Research) and platinum and silver (reference) electrodes. The reactions at the electrodes were reversible in all cases and the redox potentials were obtained as the arithmetic average of the cathodic and anodic waves. The ferrocene/ferrocenium couple (0.43 V *vs* SCE in acetonitrile, 0.1 M TBAF) was used to calibrate the reference electrode.

Results

Absorption and Fluorescence Properties. The ground-state absorption spectra recorded for NP-II and NP-III in acetonitrile are shown in Figure 3. All the naphthalidiimides studied were found to display similar absorption spectra consisting of a narrow band at 236 nm, a broad absorption band composed of a shoulder around 340–345 nm and two distinct maxima (situated at 355–365 nm and 375–385 nm, depending on the solvent used). Other higher vibronic bands are also visible between 250 and 325 nm. In addition to the 236 nm-band, all the naphthalimides exhibit a broad absorption, which is less structured than that of the naphthalidiimides and presents a maximum which is blue-shifted ($\Delta\lambda \approx 15$ nm) compared to that of the bifunctional derivatives.

In all solvents studied (benzene, dichloromethane, ethyl ether, acetone, acetonitrile, methanol, and PBS), the ground-state absorption of the naphthalenic molecules followed linear Beer–Lambert behavior in the measured range of concentrations (from 1 to 100 μM). In organic solvents, an increase in solvent polarity had no effect on the wavelength maximum of the stronger absorption at 236 nm but produced a blue-shift of the

broad band in the case of the naphthalidiimides ($\Delta\lambda = 8$ nm, from benzene to methanol) and a red-shift in the case of the naphthalimides ($\Delta\lambda = 6$ nm). These results suggest that the lowest singlet state (S_1) is mainly $\pi\pi^*$ in nature for naphthalimides whereas $n\pi^*$ character predominates for the naphthalidiimides.⁵⁵ It is worthwhile noting that the ground-state absorption properties of NP-III in aqueous buffer solution do not follow the trend observed in organic solvents: in comparison to that recorded in methanol, the spectrum of NP-III in PBS was found to be red-shifted ($\Delta\lambda = 7$ nm), indicating strong hydrogen-bonding between the molecules of NP-III and water. In the case of NP-II, as expected for a $\pi\pi^*$ singlet state, the broad absorption band undergoes a red-shift in aqueous media ($\Delta\lambda = 14$ nm, from methanol to PBS).

Figure 3 also shows the fluorescence emission spectra of NP-II and NP-III recorded in acetonitrile. These spectra, which are the mirror images of the corresponding long-wavelength absorption band, were found to be identical irrespective of the excitation wavelength used, which demonstrates the existence of only one fluorescing species. Energies of the lowest singlet state (E_S) were estimated from the overlap of the emission and absorption spectra. In the naphthalidiimide family, similar E_S values of ≈ 75 kcal mol⁻¹ were obtained whereas E_S of ≈ 80 kcal mol⁻¹ were measured in the naphthalimide series. This latter value is identical to that previously reported for *N*-methyl-1,8-naphthalimide in acetonitrile.⁵⁶ Determination of the fluorescence quantum yields of the naphthalenic derivatives in acetonitrile⁵⁷ led to Φ_f values of 0.027 and 0.147 for compound **1** and NP-II, respectively and 0.005 and 0.010 for compound **3** and NP-III, respectively. These results show the naphthalimides to be more fluorescent than the naphthalidiimides. The proticity of the solvent was observed to strongly influence the fluorescence properties of all compounds (Φ_f increases from 0.027 in acetonitrile to 0.18 in methanol to 0.44 in PBS for compound **1**, from 0.145 to 0.27 to 0.63 for NP-II, and from 0.01 to 0.04 to 0.45 for NP-III). A similar effect of the solvent proticity has already been reported in the case of several substituted and unsubstituted 1,8-naphthalimides.^{56,58–60}

Transient Absorption Spectroscopy. Figure 4A shows the transient absorption spectrum recorded at times ≥ 40 μs after laser flash photolysis ($\lambda_{\text{exc}} = 355$ nm) of NP-III, in oxygen-saturated acetonitrile. It displays negative bands with maxima around 360 and 380 nm which present a mirror image symmetry with the ground-state absorption spectrum. A large absorption band at 465 nm with a shoulder around 530 nm and other weaker bands at 600, 660, and 725 nm, which all decay following the same kinetics, are also observed. The corresponding species appears to be produced within the duration of the laser pulse and to decay slowly with a lifetime of 250–300 μs at low laser intensity. The decay of this primary long-lived species, denoted **X**, was found to become rapidly more second-order in character with increasing laser energies or ground-state concentration.

(55) The solvent shifts observed are surprising, given the rather large absorption coefficients which one would not expect from an $n\pi^*$ state. One might speculate the existence of a weaker $n\pi^*$ absorption masked by a dominant overlapping $\pi\pi^*$ absorption.

(56) Wintgens, V.; Valat, P.; Kossanyi, J.; Biczok, L.; Demeter, A.; Berces, T. *J. Chem. Soc., Faraday Trans* **1994**, *90*, 411–421.

(57) As oxygen was found to have no significant effect on the fluorescence of the naphthalenic derivatives, the Φ_f values were measured under air-saturated conditions.

(58) Barros, T. C.; Molinari, G. R.; Berci Filho, P.; Toscano, V. G.; Politi, M. *J. Photochem. Photobiol. A: Chem.* **1993**, *76*, 55–60.

(59) Samanta, A.; Saroja, G. *J. Photochem. Photobiol. A: Chem* **1994**, *84*, 19–26.

(60) The proticity of the solvent was explained to lead to a larger separation between the lowest singlet state and the lowest triplet state making the intersystem crossing less favorable while enhancing the fluorescence.

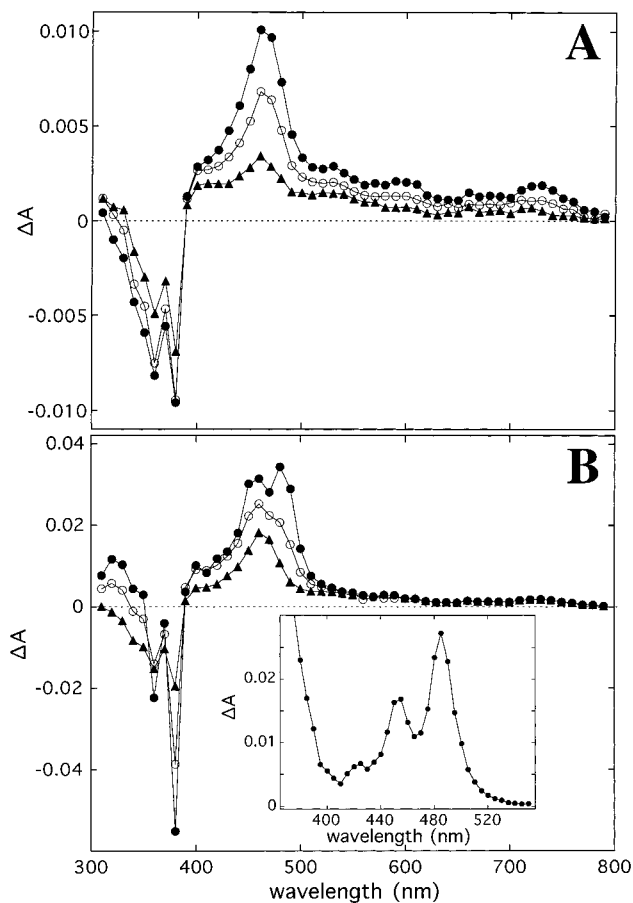


Figure 4. (A) Time-dependent transient absorption spectra recorded for NP-III in oxygen-saturated acetonitrile 40 (●), 100 (○), and 400 μ s (▲) after pulsed excitation ($\lambda_{\text{exc}} = 355$ nm). (B) Transient absorption spectra recorded for NP-III in air-saturated acetonitrile 600 ns (●), 1.5 μ s (○), and 4 μ s (▲) after the laser pulse. In both cases, the absorbance of the solution at λ_{exc} was ≈ 0.3 (corresponding to $[\text{NP-III}] \approx 15$ μM) and the laser intensity was 8 mJ cm^{-2} pulse $^{-1}$. The inset in B shows the absorption spectrum of $^3(\text{NP-III})^*$ in acetonitrile.

The absorption spectra recorded at shorter times ($t \geq 600$ ns) after 355 nm excitation of NP-III in air-saturated acetonitrile are shown in Figure 4B. This figure reveals the presence of a short-lived species in addition to the longer-lived intermediate, X. This short-lived species decays by first-order kinetics with a time constant of 450 ns. Its absorption spectrum (inset of Figure 4B) displays a band at 485 nm with a shoulder around 455 nm. The presence of a positive absorption around 325 nm in the transient difference spectrum indicates that this short-lived species has another band with a maximum at lower wavelength ($\lambda < 400$ nm).

Different behavior was observed in deaerated acetonitrile. The transient absorption spectrum recorded at times < 3 μ s after the laser pulse was identical to that of the short-lived intermediate detected in aerated solution. However, the lifetime of the corresponding species (which can be measured at 325 nm without interference from other transients) was considerably longer (7 μ s at 15 μM of NP-III) and the decay of this species was accompanied by the concomitant growth of an absorption which maximizes at 480 nm (inset of Figure 5A). In addition to the large absorption band at 480 nm, the absorption spectrum of this secondary species displays a shoulder around 530 nm and several weaker bands with maxima at 610, 680, and 760 nm (Figure 5B). This secondary species, Y, was found to decay by second-order kinetics. Following its decay, the residual

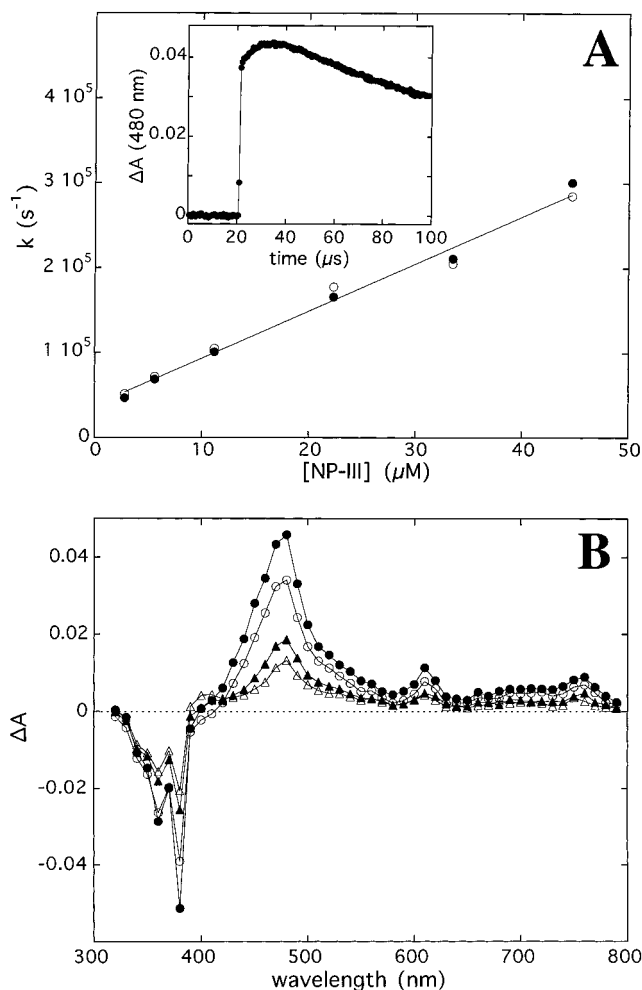


Figure 5. (A) Concentration dependence of the decay of the triplet state of NP-III monitored at 325 nm (●) and of the growth at 610 nm (○). The observed rate constants (k) were plotted against the concentration of precursor ($[\text{NP-III}]$) and the data were fitted by a linear equation. The inset shows the kinetic signal recorded at 480 nm after excitation of a solution of NP-III in deaerated acetonitrile. (B) Transient absorption spectra of the secondary long-lived species, Y, recorded 40 (●), 100 (○), 400 (▲), and 700 μ s (Δ) after the laser pulse ($\lambda_{\text{exc}} = 355$ nm). The absorbance of the solution at λ_{exc} was ≈ 0.3 ($[\text{NP-III}] \approx 15$ μM), and the laser intensity was 8 mJ cm^{-2} pulse $^{-1}$.

transient absorption spectrum was identical to that of the even longer-lived X, observed under oxygen- and air-saturated conditions.

Triplet State. The short-lived species detected in air and absorbing at 485 nm was identified as $^3(\text{NP-III})^*$, the triplet state of NP-III, through its efficient quenching⁶¹ by oxygen ($k = 2.5 \times 10^9 \text{ M}^{-1} \text{ s}^{-1}$) and 2,5-dimethyl-2,4-hexadiene ($k = 2.1 \times 10^{10} \text{ M}^{-1} \text{ s}^{-1}$) and the observation of sensitization of the triplet state absorption of perylene ($k = 1.8 \times 10^{10} \text{ M}^{-1} \text{ s}^{-1}$). $^3(\text{NP-III})^*$ was unequivocally generated by energy transfer from the triplet state of 4-methoxyacetophenone or xanthone using 266 nm as excitation wavelength (*vide infra*) and the transient absorption spectrum recorded under these conditions was found to be identical to that of the short-lived species produced by direct excitation of NP-III in aerated acetonitrile.

The lifetime of $^3(\text{NP-III})^*$ under deaerated conditions was observed to depend on the concentration of NP-III present in

(61) In these experiments, the concentration of 2,5-dimethyl-2,4-hexadiene was varied from 10 μM to 1 mM, that of perylene from 12.5 to 150 μM . The reaction rate constant with oxygen was determined using the approximations of complete removal of oxygen under N_2 -saturated conditions and a concentration of 1.9 mM in O_2 in air-saturated acetonitrile.

solution. The decay kinetics of the triplet state absorption (monitored at 325 nm) was identical to that of the growth of the secondary long-lived species at 610 nm at all concentrations of NP-III studied (between 3 and 45 μM). A plot of the observed rate constant for either of these processes against [NP-III] gave a straight line, the slope of which yields a bimolecular rate constant of $5.5 \times 10^9 \text{ M}^{-1} \text{ s}^{-1}$ (Figure 5A).

Triplet state formation was found to take place upon pulsed-excitation of all the compounds studied, *i.e.* (1) mono- and bifunctional molecules and, (2) all the *N*-substituted derivatives, irrespective of the nature of the substituent. The triplet states of all the naphthalimides have spectral features identical to those of $^3(\text{NP-III})^*$. In the case of the naphthalimides, NP-II and compound **1**, the absorption spectrum of the triplet state displays a band at 470 nm with a shoulder around 440–445 nm and another band with a maximum at lower wavelength ($\lambda < 370 \text{ nm}$).⁶² These spectral characteristics are similar to those reported for the triplet states of *N*-methyl⁵⁶ and *N*-phenyl⁶³ 1,8-naphthalimides. In a given solvent, the red-shift between the absorption of the triplet states of naphthalimides and that of the triplet states of naphthalimides parallels the red-shift of the corresponding ground-state absorptions. Triplet state formation was also observed to take place in benzene, methanol and PBS. In all cases, a decrease in solvent polarity results in a weak blue-shift of the maximum of the absorption band ($\Delta\lambda = 10 \text{ nm}$, from PBS to benzene for both the naphthalimides and naphthalimides).

The molar absorption coefficients (ϵ_T) of the triplet states of the naphthalenic derivatives were determined in acetonitrile by the sensitization method using 266 nm as excitation wavelength and 4-methoxyacetophenone as sensitizer.⁴⁷ Similar ϵ_T values were obtained for the naphthalimides ($\epsilon_T \approx 10\,500 \text{ M}^{-1} \text{ cm}^{-1}$ at 470 nm) and naphthalimides ($\epsilon_T \approx 11\,250 \text{ M}^{-1} \text{ cm}^{-1}$ at 485 nm). These values are close to that reported for *N*-methyl-1,8-naphthalimide in the same solvent ($\epsilon_T \approx 10\,000 \text{ M}^{-1} \text{ cm}^{-1}$ at 470 nm).⁵⁶

The quantum yields of intersystem crossing (Φ_{isc}) were determined by comparative actinometry using 355 nm excitation of optically-matched samples of naphthalenic derivative and benzophenone in benzene. In acetonitrile, compounds **1** and **3** were found to have quantum yields of intersystem crossing close to unity (0.95 and 1, respectively) whereas NP-II, NP-III⁶⁴ and compound **2** display lower Φ_{isc} values (0.42, 0.39, and 0.23, respectively). In PBS, where intermolecular hydrogen bonding with molecules of water is possible, Φ_{isc} was found to be reduced to 0.43 for compound **1**, 0.31 for NP-II and 0.24 for NP-III.⁶⁵

All the naphthalenic derivatives were observed to sensitize the formation of singlet oxygen, $\text{O}_2(^1\Delta_g)$. Comparison of the quantum yields of singlet oxygen production (Φ_Δ) and of intersystem crossing (Φ_{isc}) shows that in all cases, the efficiency of $\text{O}_2(^1\Delta_g)$ formation ($S_\Delta = \Phi_\Delta/\Phi_{\text{isc}}$) is high ($S_\Delta > 0.8$ for the naphthalimides and > 0.5 for the naphthalimides). Singlet oxygen was also observed to *react* with the ground-state of the naphthalenic molecules. In acetonitrile, reaction rate constants

(62) The absorption of the triplet state of compound **1** in acetonitrile is presented in Figure 8.

(63) Demeter, A.; Biczok, L.; Berces, T.; Wintgens, V.; Valat, P.; Kossanyi, J. *J. Phys. Chem.* **1993**, *97*, 3217–3224.

(64) In order to correct for the absorbance due to the primary long-lived species **X** at the λ_{max} of the triplet state, two sets of experiments were carried out: one under N_2 -saturated conditions [where both $^3(\text{NP-III})^*$ and **X** absorb], the other one under O_2 -saturated conditions (where only the primary long-lived species is produced).

(65) The Φ_{isc} determinations in aqueous media were carried out using the assumption that the triplet absorption coefficients of the naphthalenic derivatives were identical in acetonitrile and PBS.

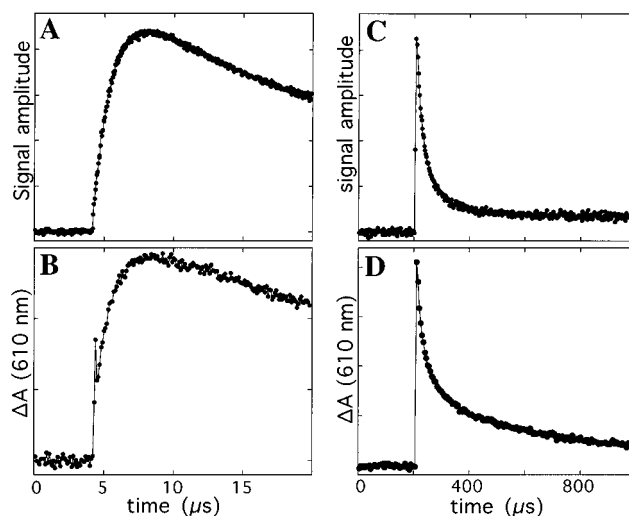


Figure 6. Transient conductivity (A and C) and transient absorption at 610 nm (B and D), recorded following pulsed excitation ($\lambda_{\text{exc}} = 355 \text{ nm}$) of NP-III in deaerated acetonitrile. The absorbance of the solution at λ_{exc} was 0.6 ([NP-III] $\approx 30 \mu\text{M}$), and the laser intensity was $10 \text{ mJ cm}^{-2} \text{ pulse}^{-1}$.

of $(2\text{--}3) \times 10^8 \text{ M}^{-1} \text{ s}^{-1}$ were determined for NP-II and compound **1** and $1 \times 10^9 \text{ M}^{-1} \text{ s}^{-1}$ for NP-III.⁶⁶

Having characterized the triplet state behavior of NP-III, we now turn our attention to the identification of the primary and secondary long-lived species, (**X** and **Y**, respectively), which are also formed on 355 nm excitation of the bishydroperoxy naphthalimide, NP-III (*vide supra*).

Secondary Long-Lived Species. In aerated acetonitrile, quenching of the triplet state of NP-III by oxygen ($k = 2.5 \times 10^9 \text{ M}^{-1} \text{ s}^{-1}$, $[\text{O}_2] = 1.9 \text{ mM}$) dominates over ground-state quenching ($k = 5.5 \times 10^9 \text{ M}^{-1} \text{ s}^{-1}$, $[\text{NP-III}] = 15 \mu\text{M}$) and the secondary species **Y** is not observed. In the absence of oxygen, however, $^3(\text{NP-III})^*$ reacts efficiently with the ground-state with a rate constant approaching diffusion control (*vide supra*) to give **Y**, the absorption spectrum of which is shown in Figure 5B.

To aid in the identification of **Y**, experiments were carried out using 355 nm excitation with simultaneous optical and conductivity detection. Figure 6 shows the time-resolved absorption (at 610 nm) and conductivity signals recorded after pulsed excitation of NP-III in deaerated acetonitrile. Good agreement was observed between the kinetics of growth of the secondary species absorbing at 610 nm (Figure 6B) and the buildup of the charged intermediate in the photoconductivity measurement (Figure 6A). The decays of the conductivity signal (Figure 6C) and of the shorter-lived species absorbing at 610 nm (Figure 6D) recorded on longer time scales also show good correspondence.⁶⁷ The obvious conclusion is that **Y** is a charged intermediate resulting from reaction between the triplet and ground-state of the bishydroperoxy naphthalimide. In aerated solution, where $^3(\text{NP-III})^*$ is exclusively quenched by oxygen, no conductivity signal could be detected. It should be noted that this experiment also leads to the conclusion that, **X**, the longer-lived species absorbing at 610 nm, is not charged.

(66) These reaction rate constants were determined by monitoring the decay of singlet oxygen phosphorescence produced by excitation ($\lambda_{\text{exc}} = 355 \text{ nm}$) of phenazine in air-saturated acetonitrile in the presence of several concentrations of naphthalenic derivatives (from 1 to $10 \mu\text{M}$). The luminescence signals were corrected for the initial fast spike due, at least in part to fluorescence of phenazine, by subtracting the signal recorded for the same solution under deaerated conditions.

(67) In addition to **Y**, the transient absorption signal recorded at 610 nm using a longer time scale (Figure 6D) presents a contribution from the primary long-lived species, **X**.

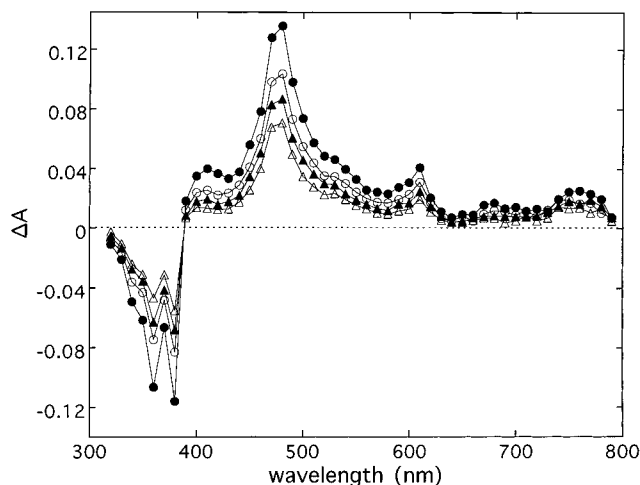


Figure 7. Transient absorption spectrum of $(\text{NP-III})^{\bullet-}$, the radical anion of NP-III resulting from reduction of the triplet state of NP-III by DABCO (100 μM). The spectra were recorded 2 (●), 15 (○), 30 (▲), and 70 μs (Δ) after the laser pulse ($\lambda_{\text{exc}} = 355 \text{ nm}$). The absorbance of the solution was ≈ 0.4 at λ_{exc} ($[\text{NP-III}] \approx 20 \mu\text{M}$), and the laser intensity was $8 \text{ mJ cm}^{-2} \text{ pulse}^{-1}$.

In order to identify **Y**, the radical anion and radical cation of the bis-hydroperoxy naphthalindiimide, were generated by independent pathways. Excitation ($\lambda_{\text{exc}} = 355 \text{ nm}$) of a deaerated solution of NP-III in acetonitrile containing the electron donor, 1,4-diazabicyclo[2,2,2]octane (DABCO, 100 μM) results in the production of a species with the absorption spectrum shown in Figure 7. This spectrum displays a large absorption band with a maximum at 480 nm, a shoulder at 530 nm and other weaker bands at 610, 680, and 760 nm.

It can be attributed to $(\text{NP-III})^{\bullet-}$, the radical anion of NP-III, formed by electron-transfer from DABCO to $^3(\text{NP-III})^*$, as described by reaction 5. In acetonitrile, this reaction was found to be diffusion controlled, by monitoring the growth of $(\text{NP-III})^{\bullet-}$ at 610 nm as a function of DABCO concentration (from 1 to 100 μM).



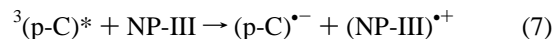
The absorption spectrum of $(\text{NP-III})^{\bullet-}$ shows the same profile as that of **Y** (Figure 5B). The absorption due to the radical cation of DABCO is very weak in this region⁶⁸ and does not contribute significantly to the observed spectrum at $\lambda > 400 \text{ nm}$. Thus, it can be concluded that the secondary long-lived species is $(\text{NP-III})^{\bullet-}$, resulting from the one-electron transfer between the ground-state and the excited triplet state of the hydroperoxy derivative, as shown in eq 6.



This reaction also leads to simultaneous production of the radical cation, $(\text{NP-III})^{\bullet+}$. However, the similarity of the absorption spectra obtained on reaction of $^3(\text{NP-III})^*$ with either DABCO or ground-state NP-III suggests that the contribution of the radical cation to the spectrum formed by the latter reaction is negligible. An attempt was made to generate $(\text{NP-III})^{\bullet+}$ through 355 nm excitation of *p*-chloranil (*p*-C) to its strongly oxidizing triplet state, which can then act as an electron acceptor in the presence of NP-III.⁶⁹

(68) Shida, T.; Nosaka, Y.; Kato, T. *J. Phys. Chem.* **1978**, *82*, 695–698.

(69) *p*-Chloranil has an E_T value^{48b} of 49.3 kcal mol⁻¹ and therefore cannot sensitize the formation of the triplet state of NP-III.



The spectrum resulting from this reaction appears to be almost exclusively that of $(\text{p-C})^{\bullet-}$, which confirms that the absorption of $(\text{NP-III})^{\bullet+}$ is very weak.⁷⁰ It is, thus, not surprising that the transient absorption spectrum observed following ground-state quenching of the triplet state is dominated by that of the radical anion, $(\text{NP-III})^{\bullet-}$. From a plot of the observed growth at 680 nm as a function of the concentration of NP-III, the rate constant for reaction 7 was determined to be $5 \times 10^9 \text{ M}^{-1} \text{ s}^{-1}$.⁷¹

In deaerated solution, the triplet states of all naphthalindiimides studied underwent electron-transfer with the ground-state, giving rise to an observable radical anion. The rate constant for this reaction (which also takes place in methanol and in water) is high (in acetonitrile, k was determined to be $4.9 \times 10^9 \text{ M}^{-1} \text{ s}^{-1}$ for compound **2**, $5.5 \times 10^9 \text{ M}^{-1} \text{ s}^{-1}$ for NP-III, and $6 \times 10^9 \text{ M}^{-1} \text{ s}^{-1}$ for compound **3** and in PBS, a k value of $3.3 \times 10^9 \text{ M}^{-1} \text{ s}^{-1}$ was obtained for NP-III).⁷² The transient absorption spectra recorded for the radical anions of these compounds were all very similar with a large absorption band at 480 nm, a shoulder at 530 nm, and several weaker bands around 610, 690, and 770 nm. The same reaction between the triplet state and the ground-state was observed to occur in the naphthalimide series. However, the rate constant of electron-transfer was found to be an order of magnitude lower ($k = 4.8 \times 10^8 \text{ M}^{-1} \text{ s}^{-1}$ for compound **1** in acetonitrile)⁷² than in the case of the naphthalindiimide derivatives. In addition, under identical conditions, formation of the radical anion of NP-II or compound **1** was less obvious in the transient absorption spectra, suggesting also a lower efficiency of the electron-transfer reaction. Similarly, the rate constant for electron-transfer from DABCO to the triplet state of compound **1** was determined to be $5 \times 10^9 \text{ M}^{-1} \text{ s}^{-1}$,⁷³ which is significantly lower than that obtained for the naphthalindiimides. The differences in the quenching of the triplet states of naphthalimides and naphthalindiimides by electron-transfer from DABCO or the corresponding ground-states, can be explained by the much more negative reduction potentials of the naphthalimides. In acetonitrile, $E_{1/2}^{\text{red}}$ values of -1.195 V vs SCE and -1.23 V vs SCE were measured for NP-II and compound **1**, respectively, whereas two reductions were observed in the case of the naphthalindiimides with, for example, $E_{1/2}^{\text{red}}$ values of -0.385 and -0.695 V vs SCE for NP-III.⁷⁴

Figure 8 shows the spectra recorded after laser flash photolysis ($\lambda_{\text{exc}} = 355 \text{ nm}$) of a deaerated solution of compound **1** in acetonitrile in the absence and presence of DABCO (1 mM). The spectrum of the radical anion of **1** is very different from that of $(\text{NP-III})^{\bullet-}$, it displays a large absorption band at 415 nm and a small shoulder around 490 nm. It is similar to that recorded for NP-II under the same conditions and to that reported for the radical anion of *N*-phenyl-1,8-naphthalimide formed by reaction with triethylamine in acetonitrile.⁶³

(70) (a) The molar absorption coefficient of the radical cation of the closely related naphthalene was reported^{70b} to be $2970 \text{ M}^{-1} \text{ cm}^{-1}$ at 685 nm. (b) Gschwind, R.; Haselbach, E. *Helv. Chim. Acta* **1979**, *62*, 941–965.

(71) At 680 nm, the absorption is mainly due to $(\text{p-C})^{\bullet-}$. However, by comparison to known radical cations of closely related compounds such as naphthalene,^{70b} a small part of the absorption at 680 nm can be due to $(\text{NP-III})^{\bullet+}$.

(72) In these experiments, the concentrations of naphthalindiimides **2** and **3** were varied from 5 to 50 μM , that of compound **1** was varied from 20 to 700 μM . In PBS, the concentration of NP-III was varied from 5 to 25 μM .

(73) This reaction rate constant was determined by monitoring the growth at 415 nm for DABCO concentrations between 5 and 500 μM .

(74) (a) The limits for the cyclic voltammetry experiments were -2 and $+2 \text{ V vs SCE}$. This explains that the oxidation of NP-III, which is expected to have a potential $> 2 \text{ V vs SCE}$ as estimated by the equation proposed by Loufty and Sharp,^{74b} was not observed. (b) Loufty, R. O.; Sharp, J. H. *Photogr. Sci. Eng.* **1976**, *20*, 165–174.

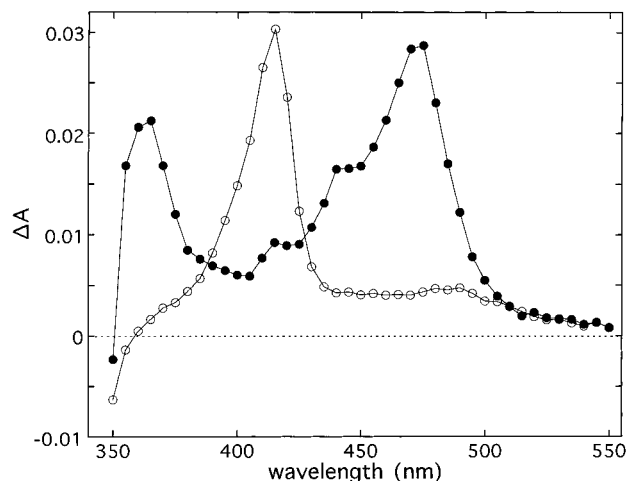


Figure 8. Transient absorption spectra of the triplet state (●) and of the radical anion (○) of compound **1** produced by electron-transfer from DABCO (1 mM) to the triplet state of the naphthalenic molecule. Each spectrum was recorded 8 μ s after laser flash photolysis ($\lambda_{\text{exc}} = 355$ nm) of a solution of **1** in deaerated acetonitrile. The laser intensity was 8 mJ cm⁻² pulse⁻¹, and the absorbance of the sample was 0.4 at 355 nm.

The radical anions of the naphthalimides and naphthalidiimides were also found to display different reactivities toward oxygen. The decay of (NP-III)^{•-} was identical under air- and N₂-saturated conditions whereas a large quenching by oxygen was observed in the case of (NP-II)^{•-}, which suggests different electron distributions in these intermediates.

By analogy with other carbonyl compounds, the high rate constant observed for electron-transfer from DABCO to the triplet state of NP-III suggests that ³(NP-III)* (as well as the triplet states of the other naphthalenic derivatives studied) behaves with typical $\pi\pi^*$ characteristics. In order to verify this statement, the reactivity of ³(NP-III)* toward hydrogen abstraction, a reaction characteristic of $n\pi^*$ ketone triplets, was examined. Relatively low rate constants for triplet quenching by known hydrogen donors such as isopropyl alcohol ($k < 1.6 \times 10^4$ M⁻¹ s⁻¹) and 1,4-cyclohexadiene ($k = 2.9 \times 10^5$ M⁻¹ s⁻¹) confirm that ³(NP-III)* is predominately $\pi\pi^*$ in nature.⁷⁵ Previous work has shown that this is also the case for a variety of naphthalimides.^{56,76}

Primary Long-Lived Species. As previously mentioned, laser flash photolysis of NP-III in acetonitrile produces a primary long-lived species, **X**, absorbing at 465 nm (see Figure 4) which appears to be formed within the laser pulse. The amplitude of the absorption, measured following decay of other transient species, is identical whether irradiation is carried out in air- or oxygen-saturated solution. It is also unaffected under conditions where the addition of quenchers such as perylene induces complete scavenging of the triplet state. These results indicate that the production of **X** is not mediated by the triplet state but more probably by the singlet state (S₁) of NP-III.

Estimations of the molar absorption coefficient, $\epsilon(\mathbf{X})$, and quantum yield of formation, $\Phi(\mathbf{X})$, of the primary long-lived species were determined in the following manner. Under oxygen-saturated conditions, **X** is the only intermediate detected at times > 100 ns (the triplet state, which is efficiently quenched by O₂, is not observed). Therefore, the spectrum recorded is the difference between the spectra of **X** and the ground-state

(75) In these experiments, the concentration of 1,4-cyclohexadiene was varied from 0.1 to 1 M and that of isopropyl alcohol was increased up to 1 M.

(76) Demeter, A.; Berces, T.; Biczok, L.; Wintgens, V.; Valat, P.; Kossanyi, J. *J. Chem. Soc. Faraday Trans* **1994**, *90*, 2635–2641.

material. The negative part in this spectrum (Figure 4A) shows a mirror image symmetry with the ground-state absorption spectrum. Under such conditions, the assumption is made that **X** does not possess significant absorption in this region and the absorbance change is a simple consequence of loss of the ground-state, which has a known absorption coefficient at 380 nm, $\epsilon(380 \text{ nm})$. The formation of **X** at the expense of the ground-state allows estimation of the molar absorption coefficient of **X** by direct comparison of the ΔA values of the signals at the depletion region and the visible absorption of the transient. Using such an approach and eq 8, an absorption coefficient of 21 600 M⁻¹ cm⁻¹ was obtained at 465 nm.⁷⁷

$$\epsilon(\mathbf{X}) = \epsilon(380\text{nm})\Delta A(465\text{nm})/\Delta A(380\text{nm}) \quad (8)$$

The quantum yield of formation of the primary long-lived species **X** was then determined by comparative actinometry using benzophenone in benzene as standard. This experiment yielded a $\Phi(\mathbf{X})$ value of 0.03.

Clues to the identity of **X** were obtained by comparison of transient absorption spectra recorded in oxygen-saturated acetonitrile for all the derivatives studied. Formation of a primary long-lived species was also observed to take place in the case of compound **2** but was not detected for any of the other naphthalidiimides or naphthalimides investigated. From a consideration of these findings and the chemical structures of these molecules, it can be concluded that the generation of a primary long-lived species requires the starting material (**1**) to be a naphthalidiimide, and, (**2**) to possess a hydrogen atom at the γ position.⁷⁸

Further information on the nature of this species was obtained from the photoconductivity experiments outlined above, which led to the conclusion that **X** is an uncharged intermediate. The decay of **X** was also found to be oxygen-independent. In the presence of the hydrogen donor, 1,4-cyclohexadiene (1,4-CHD, 500 mM), the transient absorption spectrum recorded on 355 nm excitation of NP-III in oxygen-saturated acetonitrile, showed spectral characteristics identical to those seen in the absence of 1,4-CHD, but a large increase in the signal intensity was observed. This suggests that the species produced by hydrogen abstraction from 1,4-CHD is structurally close to **X**. Under these experimental conditions, the triplet state is quenched by oxygen ($k = 2.5 \times 10^9$ M⁻¹ s⁻¹, [O₂] = 9.1 mM) rather than by the hydrogen donor ($k = 2.9 \times 10^5$ M⁻¹ s⁻¹, [1,4-CHD] = 500 mM), therefore the singlet state of NP-III is the excited intermediate involved in the hydrogen abstraction. This conclusion is confirmed by the efficient fluorescence quenching observed for NP-III in acetonitrile in the presence of 1,4-CHD (50 mM to 1 M).

Formation of the primary long-lived species was also found to take place in other solvents such as ethyl ether, acetone and methanol. The spectrum of **X** in ethyl ether was identical to that recorded in acetonitrile, whereas the spectra obtained in acetone and methanol were red-shifted and presented a large absorption band at 480 nm instead of 460 nm. Different behavior was observed in PBS, where formation of a primary long-lived species was not detected for both NP-III and

(77) This value must be viewed as a lower limit due to the assumptions made.

(78) Further evidence for the intramolecular hydrogen abstraction was obtained using *N,N'*-bis-(2-methylpropyl)-1,4,5,8-naphthalidiimide. Pulsed excitation of this molecule leads to the formation of a primary long-lived species *via* the singlet state, S₁. The absorption spectrum of the oxygen-independent species produced was observed to be similar to that generated from compound **2**. However, in the case of *N,N'*-bis(2-methylpropyl)-1,4,5,8-naphthalidiimide, the quantum yield of this photoprocess was found to be much lower than for NP-III and compound **2**.

compound **2**, suggesting that hydrogen-bonding between the naphthalenic derivatives and water inhibits the production of the primary long-lived species.

Generation of the Hydroxyl Radical ($\bullet\text{OH}$). NP-III was developed with the aim of efficient generation of the hydroxyl radical ($\bullet\text{OH}$) on near-UV irradiation. Since $\bullet\text{OH}$ exhibits negligible absorption in the visible range, its production cannot be detected by direct spectroscopic means.^{28,29} Thus, indirect trapping experiments were required to determine whether $\bullet\text{OH}$ was produced by photolysis of NP-III. *N,N*-Dimethyl-*p*-nitrosoaniline (RNO) has been used in this capacity as its reaction with $\bullet\text{OH}$ leads to the photobleaching of its characteristic 420 nm absorption band.^{79,80} Photolysis ($\lambda_{\text{exc}} = 355 \text{ nm}$) of NP-III (15 μM) in oxygen-saturated acetonitrile in the presence of RNO (50 μM) resulted in a loss of RNO absorption at 420 nm which followed first-order kinetics (the rate constant of RNO bleaching was determined to be $k = 9 \times 10^9 \text{ M}^{-1} \text{ s}^{-1}$). In order to verify that the bleaching of RNO was due to $\bullet\text{OH}$ generation (RNO also reacts with singlet oxygen) control experiments were carried out as follows. Addition of *tert*-butyl alcohol or DMSO, efficient $\bullet\text{OH}$ quenchers, resulted in the inhibition of the RNO photobleaching. Under oxygen-saturated conditions, direct reaction between $^3(\text{NP-III})^*$ and RNO was ruled out since under the same conditions, the triplet state of the structurally close compounds **2** and **3** did not show any interaction with RNO. All the above demonstrate that $\bullet\text{OH}$ is indeed responsible for the photobleaching of RNO on excitation of NP-III.⁸¹

By monitoring the magnitude of the bleached RNO absorbance at 420 nm as a function of laser intensity and carrying out comparative actinometry, the quantum yield of RNO photobleaching, and therefore that of $\bullet\text{OH}$ production, was determined to be 0.03. That $\bullet\text{OH}$ and **X** are both generated under oxygen-saturated conditions and that their quantum yields of formation are identical [$\Phi(\bullet\text{OH}) = \Phi(\text{X})$] suggest that these species are produced through the same process and have the same precursor, *i.e.* the lowest singlet state S_1 of NP-III. This conclusion is supported by the fact that in the case of the hydroperoxy derivatives, $\bullet\text{OH}$ is only detected when formation of the primary long-lived species is also observed (no RNO bleaching was seen for NP-II in acetonitrile, and pulsed excitation of NP-III in PBS, in the presence of potassium thiocyanate (KSCN) did not give rise to a detectable amount of $(\text{SCN})_2^{\bullet-}$ formed by reaction of $\bullet\text{OH}$ with SCN^- , although a lower value than 0.03 is close to our estimated detection limit for the KSCN method).⁸²

(79) Vidoczy, T.; Blinov, N. N.; Irinyi, G.; Gal, D. *J. Chem. Soc. Faraday Trans 1*, **1988**, 84, 1075–1081.

(80) Buxton, G. V.; Greenstock, W. P.; Helman, A. B. Critical Review of Rate Constants for Reactions of Hydrated Electrons, Hydrogen Atoms and Hydroxyl Radicals ($\bullet\text{OH}/\text{O}^{\bullet-}$) in Aqueous Solution. *J. Phys. Chem. Ref. Data* **1988**, 17, 523.

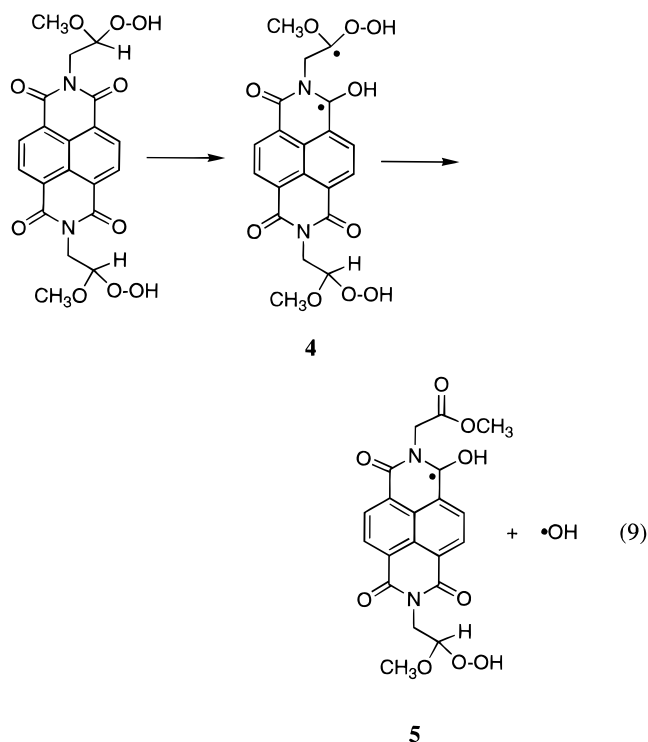
(81) From a study of the literature⁸⁰ it would appear that the rate constant for reaction between $\bullet\text{OH}$ and acetonitrile (CH_3CN) is much higher than estimated by Vidoczy *et al.* in ref 79. Under the conditions used here and in their experiments, the reaction between $\bullet\text{OH}$ and CH_3CN should occur much faster than that of $\bullet\text{OH}$ with RNO. The solvent radical species thus formed must then react with RNO resulting in its bleaching. The rate constants for reaction of $\bullet\text{OH}$ with *tert*-butyl alcohol or DMSO are higher than that for CH_3CN and at the concentrations used here, they quench $\bullet\text{OH}$ before its reaction with solvent and inhibit RNO bleaching. The reaction rate constant measured here is therefore that of the solvent radical with RNO but the quantum yield value should be correct providing all solvent radicals react with RNO. This also explains why some of the rate constants attributed to $\bullet\text{OH}$ with a variety of compounds by this method were much lower than expected.⁷⁹

(82) The lowest quantum yield of $\bullet\text{OH}$ production by direct excitation of the hydroperoxy naphthalenic derivatives was estimated to be 0.005 for the RNO method and 0.025 for the KSCN method.

Discussion

The results obtained show that the photophysical and photochemical properties of the naphthalimides (NI) and naphthaldimides (NDI) display a large, structurally-dependent variation.⁸³ A distinct difference in the absorption and fluorescence behavior is observed between the NI and NDI families. The long-wavelength absorption bands of these two series undergo opposite spectral shifts with change in solvent polarity, suggesting that the S_1 states are of different configuration. For NI, the red-shift caused by increasing solvent polarity is in accordance with a $\pi\pi^*$ configuration whereas the blue-shift in the case of NDI more resembles $n\pi^*$ behavior. This difference in electronic configuration between NI and NDI can be expected to exert a profound effect on subsequent reaction mechanisms. Confirmation is provided by the fact that among the molecules bearing a hydrogen atom at the γ position relative to the carbonyl group, intramolecular hydrogen atom abstraction was only seen to occur in the NDI compounds (NP-III and compound **2**) but not in NP-II.

On excitation of NP-III and compound **2**, a primary long-lived species was observed to be formed and was demonstrated to arise from the S_1 state of the NDI. The photochemistry of NP-III showed that the hydroxyl radical was produced from the S_1 state with a quantum yield identical to that of **X**, suggesting a common pathway for the formation of these two intermediates. A plausible mechanism for the generation of $\bullet\text{OH}$ involves the intramolecular γ hydrogen abstraction to generate the 1,4-biradical **4** followed by cleavage of the hydroperoxy bond to give $\bullet\text{OH}$ and the ketyl radical **5**, as shown by eq 9.

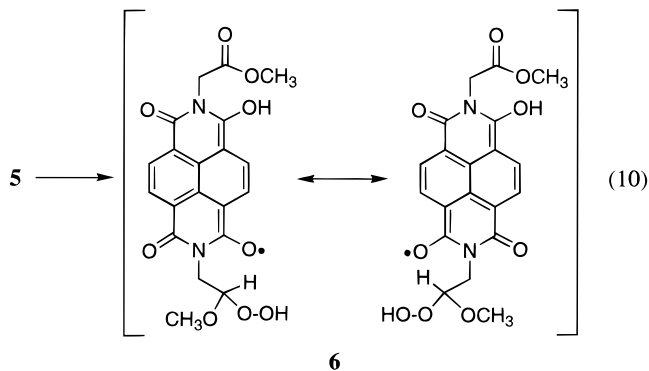


These two processes (intramolecular hydrogen abstraction and O-OH bond cleavage) are both very rapid and the 1,4-biradical **4** is not observed with the detection system used in this study. This is not surprising since singlet biradicals are expected to have very short lifetimes.⁸⁴ Ketyl radicals such as **5** are

(83) A discussion of the differences between the photoproperties of NI and NDI molecules will be published elsewhere. Here we wish to discuss these differences in view of their consequences in the biological applications of these compounds.

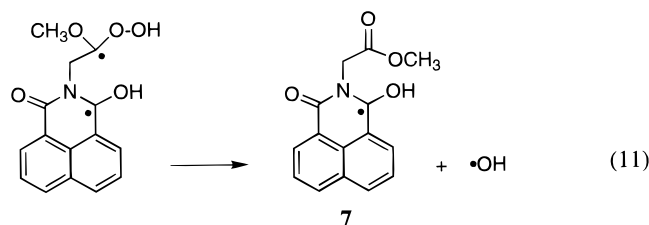
(84) Johnston, L. J.; Scaiano, J. C. *Chem. Rev.* **1989**, 89, 521–547.

normally very reactive toward oxygen. One explanation for the lack of oxygen reactivity observed for **X** is the rearrangement shown in eq 10 to give the oxygen-centered radical **6**.⁸⁵



A similar mechanism involving hydrogen abstraction and O-OH bond cleavage as a source of $\cdot\text{OH}$ was previously suggested for NP-III but proposed $^3(\text{NP-III})^*$ as the precursor.²² The experiments reported here provide a refinement of the mechanism to involve the singlet state rather than triplet state as the excited state intermediate responsible for $\cdot\text{OH}$ generation.

The naphthalimide analog NP-II does not exhibit formation of such a primary long-lived species in aerated acetonitrile, even though a γ hydrogen is available. There are three possible explanations for this behavior: (1) the $\pi\pi^*$ nature of the S_1 state of NP-II reduces the efficiency of this reaction compared to the $n\pi^*$ S_1 state of NP-III, (2) the hydrogen abstraction occurs and the 1,4-biradical is formed but it then collapses back to the starting material or gives cyclic products, (3) hydrogen abstraction takes place but the resulting 1,4-biradical and subsequent products are transparent at $\lambda > 300$ nm. The absence of hydroxyl radical generation from NP-II suggests that (1) and/or (2) applies. The product of an intramolecular γ hydrogen abstraction reaction and subsequent $\cdot\text{OH}$ liberation would be **7**, which is a ketyl radical and should be detectable, as would the liberated $\cdot\text{OH}$.



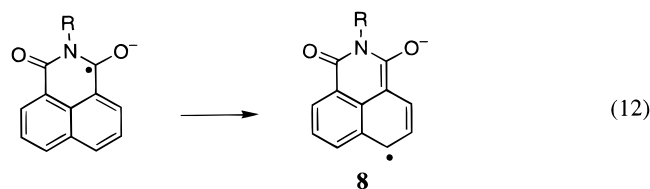
The triplet states of both NI and NDI compounds behave in a similar manner, typical of a $\pi\pi^*$ configuration. Electron-transfer reactions were observed to be very efficient between all triplet states and electron donors such as DABCO. Additionally, these triplet states are relatively unreactive toward hydrogen abstraction, even with excellent hydrogen donor molecule like 1,4-CHD ($k = 2.9 \times 10^5 \text{ M}^{-1} \text{ s}^{-1}$ for NP-III in acetonitrile). This rate constant can be equated to that exhibited by a true $n\pi^*$ triplet state such as that of benzophenone for example (for which, in acetonitrile, a k value of $2.9 \times 10^8 \text{ M}^{-1} \text{ s}^{-1}$ was reported for hydrogen abstraction from 1,4-CHD).⁸⁶

The radical anions of NI and NDI display very different absorption spectra (see Figures 5B and 8). They also display different reactivity toward oxygen: $(\text{NP-III})^{\bullet-}$ was found to be

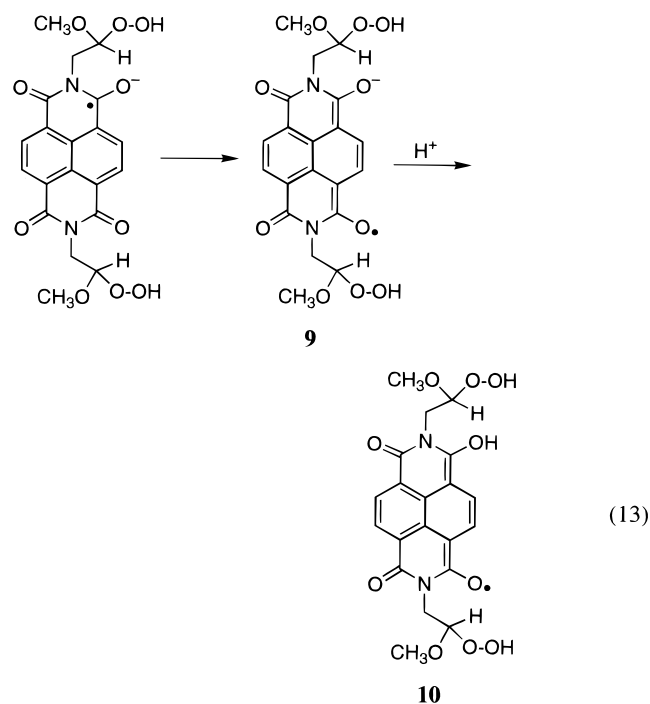
(85) It is worthwhile noting that two structures can be drawn, one where the radical is localized at the oxygen atom in the 4 position and the other where the radical is borne by the oxygen atom in the 5 position.

(86) Encinas, M. V.; Scaiano, J. C. *J. Am. Chem. Soc.* **1981**, *103*, 6393–6397.

unaffected by O_2 whereas the radical anion of NP-II is very oxygen sensitive. The radical anions of related *N*-substituted 1,8-naphthalimides studied by Berces and co-workers⁷⁶ exhibit spectra similar to that of $(\text{NP-II})^{\bullet-}$ and are proposed to have the structure shown in **8**, based on theoretical calculations. The presence of a carbon-centered radical in this intermediate explains the reactivity toward oxygen.

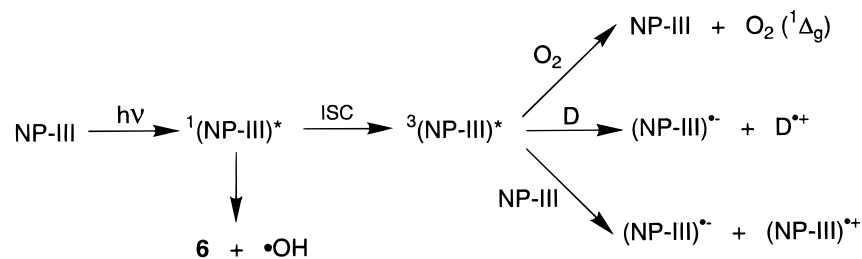


In the case of $(\text{NP-III})^{\bullet-}$, rearrangement may again occur along the extended molecule to give the oxygen-centered radical anion **9**. Supporting evidence for this assignment comes from the absence of reactivity toward oxygen and the fact that addition of a few drops of HCl to a deaerated solution of NP-III in acetonitrile results in a change in the spectrum of $(\text{NP-III})^{\bullet-}$ to a spectrum more in agreement with **X** produced from excitation of NP-III in aerated acetonitrile. Protonation of $(\text{NP-III})^{\bullet-}$ would give **10**, the chromophore of which is essentially the same as that of **6**.



Given the versatility of NI and NDI molecules in biological applications, it is of interest to compare the mechanistic photochemistry presented here with the observed photobiological effects of these compounds in order to arrive at informed speculations concerning the mechanistic basis of the biological phenomena. Triplet state formation is an efficient process in NP-III ($\Phi_{\text{isc}} = 0.39$ in acetonitrile and 0.24 in PBS) and various reactions can take place from this state. In the presence of oxygen, energy transfer to O_2 leads to the formation of singlet oxygen ($\text{O}_2, ^1\Delta_g$) with high efficiency for such $\pi\pi^*$ triplet states and as this species is highly oxidative, Type II biological damage may ensue in the presence of suitable substrates. Alternatively, it has been demonstrated that $^3(\text{NP-III})^*$ is both a strong pro-oxidant and reductant in one-electron transfer reactions and Type

Scheme 1. Possible Excited State Decay Channels for NP-III in the Presence and the Absence of an Electron-Donor Molecule, D



I biological damage⁸⁷ may be induced in this fashion. Singlet state reactions also lead to the formation of reactive intermediates which must be considered in context of reactions in biological media. Intramolecular hydrogen abstraction and subsequent rearrangement give rise to hydroxyl radicals (one of the most oxidative species known) and other free radical species. Clearly then, NP-III is a highly photoreactive molecule, capable of functioning by various means *via* oxygen-dependent and oxygen-independent mechanisms.

Both NP-II and NP-III have been shown to induce sequence-specific photonuclease activity by initiating piperidine-assisted cleavage of DNA at the 5'G of 5'-GG-3' sequences.^{20,21} Both hydroxyl radical formation and electron-transfer reactions from guanine residues have been proposed to be responsible for this effect. Our results clarify this situation as NP-II does not produce detectable levels ($\Phi < 0.005$) of $\bullet\text{OH}$, in contrast to NP-III. Guanine is the most easily (one-electron) oxidized base and is a good electron donor which reacts readily with the triplet state of NP-II ($k = 3.6 \times 10^8 \text{ M}^{-1} \text{ s}^{-1}$) and that of NP-III ($k = 2.5 \times 10^9 \text{ M}^{-1} \text{ s}^{-1}$) in PBS, in the form of guanosine. The electron-transfer reaction can be considered the most likely pathway for this reaction given the 5'-GG-3' sequence selectivity which has been shown to be typical of electron acceptor photonucleases such as methylene blue⁸⁸ and anthraquinone derivatives,^{89,90} in contrast to the random cleavage patterns produced by other $\bullet\text{OH}$ generating systems.⁹¹ This selectivity has been explained recently to be due to the 5'G of 5'-GG-3' to be the most electron donating site in DNA and subsequent acts as a "hole" sink.⁹² In model systems both NP-II and NP-III were shown to generate 8-hydroxyguanosine (8-OHdG) from irradiation in the presence of guanosine, the efficiency of this reaction being much higher for NP-III than NP-II.²¹ 8-OHdG is a fairly nonspecific mechanistic indicator as it has been demonstrated to arise from reaction of guanine with $\bullet\text{OH}$, $\text{O}_2(^1\Delta_g)$ and by one-electron oxidative reactions.⁹³ Saito and co-workers have demonstrated the efficacy of a 1,8-naphthalimide derivative containing no hydroperoxy group in the *N*-substituent in generating sequence-specific cleavage at 5'G of 5'-GG-3' sites. Obviously, $\bullet\text{OH}$ cannot be involved in this reaction and electron-transfer from guanine is probable.

(87) Foote, C. S. *Photochem. Photobiol.* **1991**, *54*, 659.

(88) Schneider, J. E.; Price, S.; Maidt, L.; Gutteridge, J. M. C.; Floyd, R. A. *Nucleic Acids Res.* **1990**, *18*, 631–635.

(89) Armitage, B.; Yu, C.; Devadoss, C.; Schuster, G. B. *J. Am. Chem. Soc.* **1994**, *116*, 9841–9889.

(90) Breslin, D. T.; Schuster, G. B. *J. Am. Chem. Soc.* **1996**, *118*, 2311–2319.

(91) Portugal, J.; Waring, M. J. *FEBS Lett.* **1987**, *225*, 195–200.

(92) Sugiyama, H.; Saito, I. *J. Am. Chem. Soc.* **1996**, *118*, 7063–7068.

(93) Kasai, H.; Yamaizumi, Z.; Berger, M.; Cadet, J. *J. Am. Chem. Soc.* **1992**, *114*, 9692–9694.

Bromo-substituted naphthalimides have been used in the neutralization of viruses such as herpes simplex and HIV-1 to sterilize blood and blood products.^{7–9} The same types of compounds have also been shown to induce tissue repair on irradiation with visible light (420 nm).^{13,14} In blood purification, the photodynamic reaction can be mediated by either singlet oxygen or by electron-transfer with viral protein leading to denaturation and loss of protein function. Preliminary indications of oxygen independence suggest the latter effect to be effective although the contribution of the singlet oxygen pathway leading to protein damage and inactivation cannot be discarded under the conditions normally needed for such a procedure. In the tissue welding application, the formation of cross-linked collagen appears to be necessary to impart strength to the weld. Although singlet oxygen has been proposed to initiate crosslinking in proteins, it is likely that the bis-naphthalimides used are reacting directly with collagen at both reactive "ends" to form a bridged crosslink. This reaction is likely of an electron-transfer nature with available electron rich amino acids in the collagen since the bisnaphthalimides were shown to be reactive toward tryptophan, tyrosine, methionine, and cysteine in an oxygen-independent manner.

Conclusion

This work has shown the mechanistic basis for the varied uses of naphthalenic imides in photobiological applications. These compounds can interact *via* oxygen-dependent and/or oxygen-independent mechanisms, thus, overcoming a potential limitation to their use in photodynamic applications. Subtle changes in the electronic character of the lowest excited states have large effects on the photochemistry of these compounds. NP-III, was confirmed to be a hydroxyl radical photogenerator, although not in a specific fashion. However, alternative reaction mechanisms such as singlet oxygen sensitization and electron-transfer ability, provide this compound with a strong arsenal of reactivity with which to affect and alter biological systems. The reaction mechanisms operating in such milieu will likely be determined by the environment of the compound and the accessibility of reactive substrates for each pathway (Scheme 1).

Acknowledgment. We gratefully acknowledge Susan Blood from the Worcester Polytechnic Institute (Worcester, MA) for assistance in the cyclic voltammetry measurements. This work was supported by the MFEL program of the ONR under Contract N00014-94-1-0927.

JA971993C